

A Micromechanics Approach to Residual Life Assessment of Nickel-Based Superalloys

H.C. Basoalto¹, A. Wisbey² and J.W. Brooks¹

¹*Cody Technology Park, QinetiQ plc, Farnborough, Hampshire, GU14 0LX, United Kingdom*

²*Serco Assurance, Thompson House, Birchwood Park, Warrington, Cheshire, WA3 6AT, United Kingdom*

Abstract

The need to drive down the operating cost of aero-engines has led to increased interest in failure prediction and life extension of components in gas turbines. The aim of this paper is to present a generic microstructure-based remnant life assessment method for nickel-based superalloys, built upon an understanding of the dominant damage micromechanisms. Mechanical testing has been carried out on two superalloys (conventionally cast IN738LC and the single crystal CMSX4) to assess the effects of strain and thermally-induced damage. The microstructural re-arrangements accompanying creep and fracture have been studied using FEG-SEM and the results obtained have been used to develop a microstructure-explicit deformation model that links microstructural evolution to the macroscopic behaviour. The model predictions are in good agreement with experiment in terms of the strain accumulation and microstructural changes. Thus, the proposed approach provides a potential framework for developing a valuable tool in undertaking remnant life assessment.

1 Introduction

Creep of nickel-based superalloys is a physical phenomenon associated with the movement of dislocations. The presence of heterogeneous structures, such as second phase particles, make the motion of dislocations difficult as they pin dislocation line segments, thereby, hindering further movement. At temperatures greater than 0.4 of the melting temperature, thermal agitation of the lattice provides the driving force necessary for non-conservative dislocation motion at stresses below yield, where trapped dislocations can climb onto an adjacent slip plane and by-pass the obstacles locally. The creep rate is then controlled by how fast dislocations can escape such pinning obstacles. This is the origin of the time dependence of creep in precipitate strengthened materials.

The microstructures of cast nickel alloys are not in thermodynamic equilibrium and consequently will undergo a number of irreversible microstructural rearrangements during service that will affect the overall creep performance. These instabilities can be strain, thermally and environmentally induced, and they all have the effect of increasing the rate at which creep damage accumulates [1,2]. Thus, creep damage not only refers to the presence and growth of voids and cracks, as proposed by Kachanov and Rabotnov [3, 4], but, is extended to include

any micromechanism that accelerates the creep rate. A number of damage micromechanisms (i.e., changes in the microstructure during service) can operate in nickel-based superalloys over the stress/temperature conditions of interest. The aim of this paper is to provide a sound understanding of the basic material degradation behaviour that affects life in terms of damage and how such information can be used to develop a microstructure-explicit damage lifing model for precipitate strengthened alloys.

2 Experimental Procedure

The two nickel-based superalloys under consideration are: the second generation single crystal CMSX4 and the conventionally cast low carbon IN738LC alloy. The CMSX4 test bars were nominally oriented so that the bar longitudinal axis, was approximately parallel to the <001> crystallographic orientation in the single crystal. The composition and heat treatment of the two alloys is shown in Table 1. All creep tests have been conducted to BS10291, with 3 thermocouples attached to the gauge length and extensometry positioned on the samples to monitor the strain time behaviour. All tests have been performed under constant load conditions.

Table 1 The composition (all wt.%) and heat treatment of the CMSX4 and IN738LC alloys.

Alloy	Cr	Co	Mo	W	Ta	Al	Ti	Re	Others
CMSX4	6.4	9.7	0.6	6.4	6.5	5.6	1.0 4	2.9	0.01Nb-0.038Fe-0.003C-0.002B-0.001Zr-0.11Hf, balance Ni
IN738LC	16	8.5	1.8	2.6	1.8	3.5	3.5	-	0.9Nb-0.04Fe-0.09C-0.01B-0.1Zr, balance Ni
Heat Treatment									
CMSX4	1315°C (6 hours) gas cool + 1140°C (6 hours) gas cool + 870°C (20 hours) air cool								
IN738LC	1120°C (2 hours) air cool + 840°C (24 hours) air cool								

The samples of both alloys were isothermally exposed between 750-1050°C for 500-10000 hours. The samples were mechanically polished (the transverse plane, perpendicular to the long axis of the test bars) and electrochemically etched in a solution of 2% phosphoric acid in water. The samples were then examined with a Field Emission Gun Scanning Electron Microscope (FEG-SEM) using a back-scattered imaging method. The images were analysed using ImageJ software.

3 Results

3.1 Isothermal Exposure

FEG-SEM analysis of the as-received (i.e. fully heat treated and ready for service) CMSX4 sample showed the expected microstructure dominated by cuboidal γ' precipitates, which are 0.32-0.39 μm in size, see Figure 1. The microstructural evolution of the thermally exposed CMSX4 samples at 850, 950 and 1050°C are also shown in Figure 1 at 500, 2500, 5000 and 10000 hours. The FEG-SEM

images clearly show how the initial γ' dispersion changes from cubic particles to a rafted structure, with the changes occurring at shorter times with increasing temperature. It is worth noting that at 1050°C the microstructure becomes inverted, with the γ' phase forming the matrix, with γ particles within it.

The conventionally cast nickel-based superalloy IN738LC is a 45-50% γ' volume fraction superalloy with an average grain size of about 1 μm . The as-received γ' dispersion is characterised by a bi-modal particle distribution of primary and secondary γ' particles as shown in Figure 2. FEG-SEM images of the coarsening of the γ' phase during thermal exposure between 500 to 10000 hours at 750, 850 and 950°C are presented in Figure 2. At 850°C the secondary γ' distribution has disappeared after 2500 hours, after which the alloy has a unimodal distribution of γ' particles. At 950°C the secondary γ' distribution has disappeared after 500 hours and some coarsening of the primary γ' particles appears to be occurring.

3.2 Creep Response

Figure 3 shows normalised CMSX4 $\langle 001 \rangle$ creep curves generated at two different stress/temperature conditions and it can be seen that the shape of the strain-time trajectories is primary creep dominated at low temperatures (750°C-800°C) but displays tertiary dominated behaviour at intermediate and high temperatures (>800°C). These differences are a reflection of the alternative micromechanisms operating at low and high temperatures. Two important damage mechanisms, generic to the nickel alloys, are the coarsening of the γ' particles and the multiplication of dislocations in the austenitic γ nickel matrix [2].

The strain-time trajectories of material that had been subjected to thermal exposure for 5000 hours at 750°C and 950°C, prior to creep testing at 850°C and 675MPa may be seen in Figure 4. These rupture test conditions were selected to give a life of approximately 100 hours in virgin material and clearly the material given the thermal exposure at 750°C has experienced little or no change in creep performance. This is consistent with expectations for thermal exposure at such a low relative temperature. However, the material exposed at 950°C for 5000 hours showed a dramatic reduction in rupture life, with a time to failure of ~20 hours.

The creep behaviour of this conventionally cast superalloy is very different from that of the single crystal nickel-based superalloy CMSX4. The main features to observe are that the creep behaviour of IN738LC is characterised by small primary transients followed by a dominant secondary stage for all temperatures investigated, see Figure 5. For the 150 MPa at 950°C creep tests (Figure 5) the creep ductility was low (at ~0.8%). This behaviour has been reported in the literature to be due to the growth of grain boundary voids/cavities by stress-directed diffusion of vacancies along the boundaries [2]. However, further fractographic analysis of this sample is needed to eliminate the presence of casting porosity as a further cause of low strains to failure.

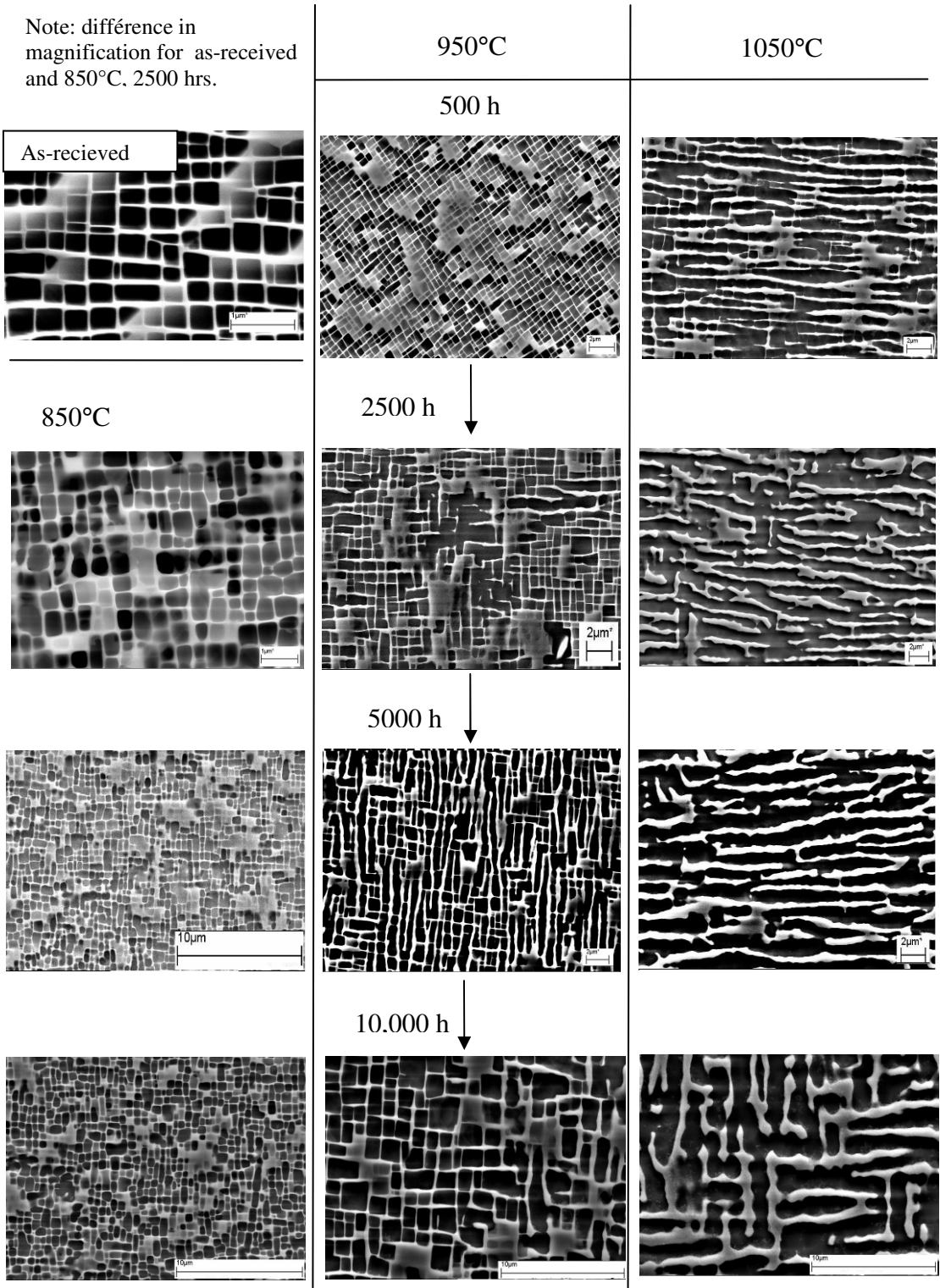


Figure 1 FEG-SEM images of thermally exposed CMSX4 at 850, 950 and 1050°C. All images are of approximately equal magnification, except where stated.

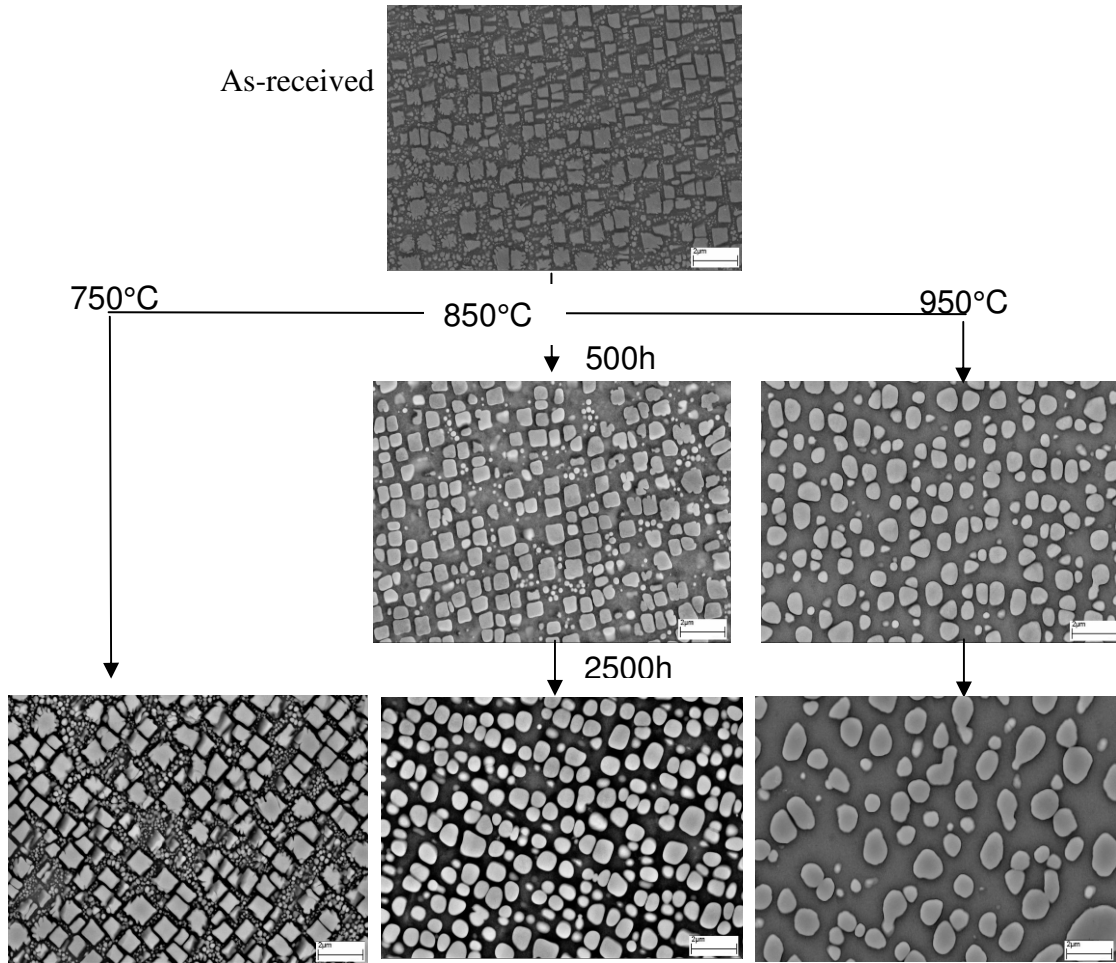


Figure 2 FEG-SEM images of thermally exposed IN738LC samples at 750, 850 and 950°C.

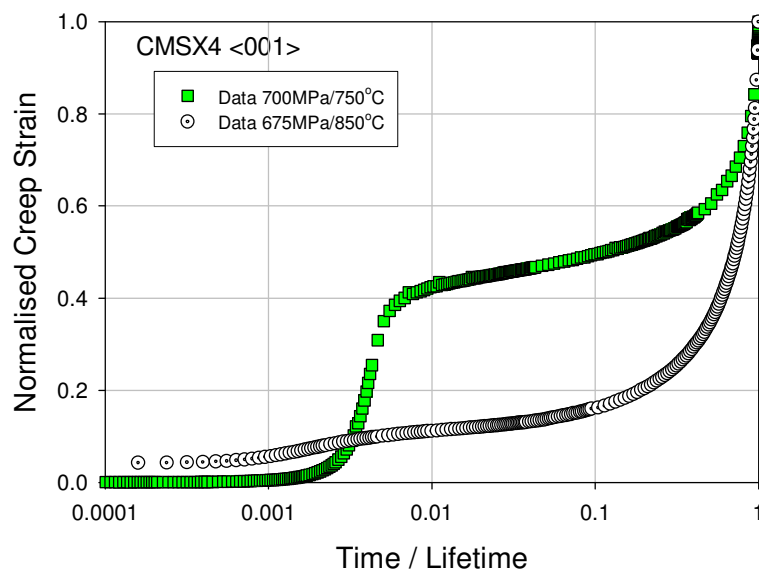


Figure 3 Creep response of CMSX4 showing very different shapes of creep curve.

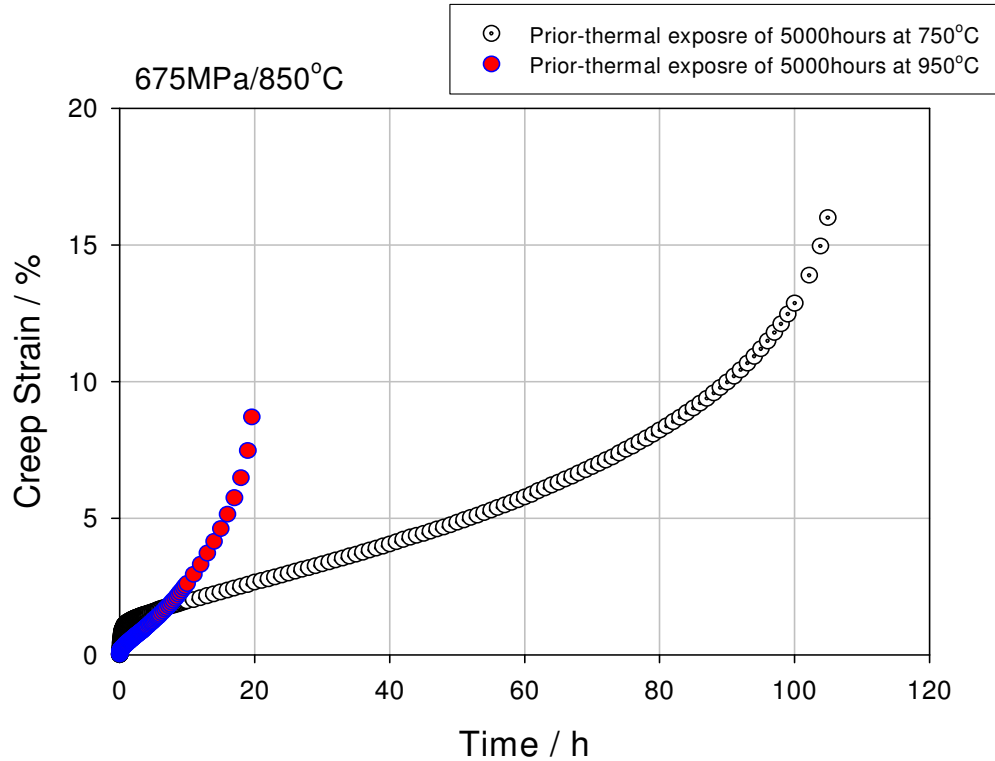


Figure 4 CMSX4 <001> creep response at 675MPa/850°C after 5000 hours thermal exposure at 750 and 950°C.

4 Discussion

4.1 CMSX4

From Section 3, it is clear that the creep response is sensitive to the initial microstructure of the material. Thermal exposure of CMSX4 at 750°C and 950°C for 5000 hours will result in two very different microstructures, see Figure 4. Creep testing at 675 MPa/850°C of these samples showed how the rafted structure resulted in a much weaker material in creep, with a reduction in life by a factor of ~5, as well as, a reduction in the extent of primary creep. It is possible to rationalise these findings by the following physical arguments, which have been formalised into a model. It should be noted that this model was developed for nickel base alloys with a lower γ' volume fraction and finer dispersoids than seen with the CMSX4, however, the model does provide a starting point for understanding the data obtained. Creep of precipitate strengthened alloys is a thermally activated process, whereby dislocations pinned by particles overcome them non-conservatively by climb. Dyson [7] has developed a microstructure-explicit approach to modelling creep of precipitate strengthened alloys, which predicts the following relationship between the creep rate, $\dot{\epsilon}$, and microstructure:

$$\dot{\epsilon} = \frac{1.6\rho_m \phi_p}{M} \left(\sqrt{\pi/4\phi_p} - 1 \right) D_v c_j \sinh \left(\frac{(\sigma - \sigma_k) b^2 \lambda_p}{kT} \right) \quad (1)$$

where ρ_m is the mobile dislocation density, D_v is the diffusivity, c_j concentration of vacancies, σ the applied stress, σ_k a kinematic back stress resulting from stress transfer between the γ matrix and γ' particles, ϕ_p the γ' volume fraction, λ_p the inter-particle spacing, b the Burger's vector, k Boltzmann's constant, T the applied temperature and M the Taylor factor. For two initial microstructures '1' and '2', which have different inter-particle spacing such that $\lambda_{p,1} > \lambda_{p,2}$, then from Equation (1) it follows the creep rate for the coarser material (larger inter-particle spacing) will be greater than that with the smaller inter-particle spacing. From these theoretical considerations it is expected that thermal exposure of a precipitate strengthened material will result in poorer creep performance, since the particles will coarsen. The creep test results of thermally exposed CMSX4 (Figure 4) could be understood on the basis of these arguments. It follows from thermal exposure experiments with zero stress presented in Section 3 (see Figure 1) that the coarsening kinetics at 750°C for CMSX4 are too slow to alter the γ' dispersion significantly. However, care must be taken when dealing with CMSX4 as the γ' particles after 5000 hour thermal exposure at 950°C have clearly formed a rafted structure. However, from image analysis of the γ' dispersion the inter-particle spacing between the γ' rafts (~0.7-0.8 μm) at 950°C is greater than that of the cuboidal structure (~0.5 μm) at 750°C. Thus the arguments noted above could still apply.

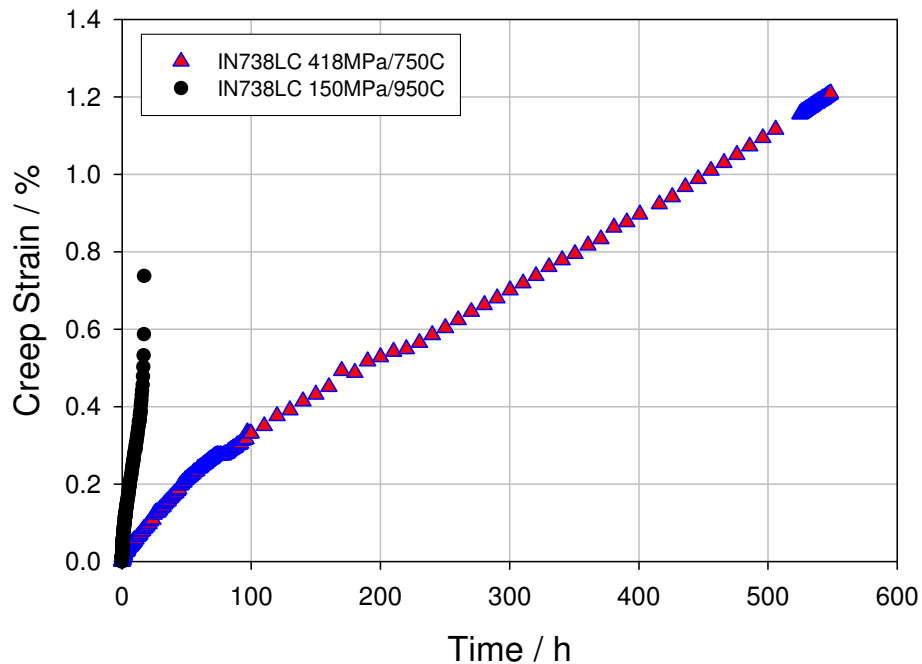


Figure 5 Creep behaviour of IN738.

4.2 IN738LC

Here the microstructural changes do not appear to be quite as dramatic as with the CMSX4, however, the primary γ' particles change from an initial cuboidal shape to spherical particles (Figure 2) and an initial bimodal distribution may become unimodal under some thermal conditions (high temperatures). These changes may be well understood with conventional particle growth and dissolution concepts, as noted elsewhere.

For the conventionally cast alloy IN738LC the shapes of the curves do not vary as dramatically as those found in CMSX4 and show the classical primary, secondary and tertiary transients [2]. For the creep tests conducted so far, two have been interrupted. As already noted in Section 4.3, the 150 MPa/950°C rupture test, the creep curve is dominated by secondary creep followed by a relatively short tertiary stage. The low ductility (<1%) is consistent with failure being by creep fracture, where voids grow by stress-directed diffusion of vacancies along grain boundaries. If this is shown to be the case then failure occurs when the voids link up thereby totally separating the adjacent grains. The void growth rate is dependent on the constraining effects of the surrounding non-cavitated grains, which in turn depends on how they are deforming. At high stresses the creep rate in the surrounding uncavitated material can become high enough to be able to accommodate the additional strains of the cavitated grains. As the stress decreases the creep rate in the surrounding material drops and so it becomes more difficult for the system to locally accommodate the addition strains around the cavitated grains. This gives rise to either unconstrained or constrained growth behaviour dependent on the deformation conditions [8].

4.3 Modelling Remnant Life

This section briefly outlines the mathematical framework for the microstructurally explicit model. Thus this links the material re-arrangements at the micro-scale to its macroscopic behaviour (i.e., its creep) and this is based on the evolution of state variables. These variables are continuum representations of the mean or expectation value of a physical quantity that affects the strain rate or stress at a material point. This approach was originally pioneered by Ashby and Dyson within a phenomenological damage mechanics framework [9], which has been extended by Dyson et al. [2] into a microstructure-explicit state variable approach. The model requires an explicit expression for the creep rate based on the stress and microstructure and evolution equations for the state variables representing the microstructure. The form of these evolution equations will depend on the physical micromechanisms that are operating. Such an approach will, therefore, lead to a coupled set of differential equations, such as [2, 10]:

$$\dot{\epsilon} = \dot{\epsilon}(\sigma, T, \rho_m, \lambda_p, \phi_p, \dots) \quad (2)$$

$$\dot{\rho}_m = \dot{\rho}_m(\sigma, T, \rho_m, \lambda_p, \phi_p, \dots) \quad (3)$$

$$\dot{\lambda}_p = \dot{\lambda}_p(T, \lambda_p, \phi_p) \quad (4)$$

$$\dot{\phi}_p = \dot{\phi}_p(T) \quad (5)$$

where σ is the applied stress, ρ_m is the mobile dislocation density, λ_p the inter-particle spacing, ϕ_p the volume fraction and T the applied temperature. The mathematical structure presented above establishes a link between the macroscopic response (the creep rate) and the evolving microstructure.

To date this model has been successful at capturing the behaviour of the conventionally cast IN738LC and good progress is being made in developing the model for single crystal nickel alloys, like CMSX4.

6 Conclusions

A range of mechanical testing and microstructural investigations have been performed to assist in understanding the degradation mechanisms occurring in two cast nickel base alloys, used in aero-engines – the single crystal nickel alloy, CMSX4 and the conventionally cast nickel alloy, IN738LC. It has been shown that these materials can display a range of creep deformation behaviours under differing conditions and also that the microstructure of the alloys is unstable at the likely operating temperatures to be seen in service. Thus the remnant life assessment of hot gas path components from aero-engines is a complex multi-faceted problem but is an important capability that is required to enable the safe and economic re-use of ex-service components and hence reduce through life costs.

The creep and microstructural data generated in this work has assisted in defining an approach for a practical remnant life assessment method, based on the dominance of creep damage. In addition to the creep damage work a very limited study into the effects on fatigue has also been commenced and this suggests that there is a reduced life after a prior creep exposure.

A physics-based model that captures the strain accumulation and the microstructural changes during creep will be a valuable tool in undertaking the remnant life assessment and some of the data generated in this work will contribute to the development. The approach currently being developed by Dyson and co-workers [2,7] provides a possible framework that brings microstructural changes into a continuum damage mechanics formulation.

Acknowledgements

This work was carried out as part of MoD (TA/N05507) and TSB (TP/5/MAT/6/I/H0101B) funded programmes. The authors are particularly grateful to Dr. P. Holdway for providing the SEM images and to R.Savage, W.Mitten and M. Sumner for carrying out the testing.

References

1. M.F. Ashby and B.F. Dyson, Creep damage mechanics and micro-mechanisms, *Advances in Fracture Research*, Ed. by Valluri et al., Pergamon Press, 1, pp. 3-30, 1984.
2. H. Basoalto, S. Sondhi, B.F. Dyson and M. McLean, A generic microstructure-explicit model of creep in nickel-based superalloys, *Superalloys 2004*, Ed. K Green et al, TMS, pp. 897-906, 2004.
3. L.M. Kachanov, On creep rupture time, *Izv. Ak. Nauk SSSR Otdel. Tekh. Nauk* 8, pp. 26-31, 1958.
4. Y.N. Rabotnov, Creep problems in structural members, *Proc. XII IUTAM Congress*, Stanford, Ed. Hetenyi & Vincenti, Springer, pp. 137, 1969.
5. I.M.Lifschitz, V.V.Slyozov, *J. Phys. Chem. Solids*, Vol. 19, 1961, pp.35.
6. P.C.Xia, J.J.Yu, X.F.Sun, H.R.Guan, Z.Q.Hu, The influence of thermal exposure on the microstructure and stress rupture property of DZ951 nickel-base alloy, *J. Alloys & Comps.*, vol. 443, 2007, pp. 125-131.
7. B.F. Dyson, A Microstructure-Based Creep Constitutive Model for Precipitation-Strengthened Alloys: Theory and Application, submitted to *Journal Materials Sci. Tech.*, 2008.
8. B.F. Dyson, Constraints on diffusional cavity growth rates, *Metal Sci.*, 10, pp. 349, 1976.
9. H. C. Basoalto, Improved Modelling of Material Properties for Higher Efficiency Power Plant (IMMP3), TSB Project No. TP/5/MAT/6/I/H0101B.
10. M.F. Ashby, and B.F. Dyson, in *Advances in Fracture Research*, Ed by Taplin et al., p.30, Pergon Pressm Oxford, 1984.
11. B.F. Dyson, and M. McLean, Microstructural Stability of Creep Resistant Alloys for high Temperature Plant Application, Ed. A. Strang et al., *The Institute of Materials*, 1998.